



5-2-13

UPTHROW OF RIGID BLOCKS DUE TO STRONG GROUND SHAKING

Benito M. PACHECO¹ and Yozo FUJINO²

¹Department of Civil Engineering, University of Tokyo, Tokyo, Japan

²Engineering Research Institute, University of Tokyo, Tokyo, Japan

SUMMARY

Small boulders were reported upthrown in the Western Nagano, Japan earthquake of 1984 (M=6.8). Many stones were found displaced so much that "anomalous" high accelerations (5-30 g) might be surmised (Ref. 1). In the present paper, a simplified model is discussed that may explain upthrow-related displacements in terms of ground accelerations not substantially exceeding 1 g. Boulder is modelled as rigid block; ground as unbonded vertical and horizontal springs and dashpots at the block's base; and ground motion as vertical and horizontal random accelerations. Example simulations indicate that ground motion features such as large horizontal pulses are also necessary in causing upthrow and large horizontal displacements of small blocks.

INTRODUCTION

In Ref. 1, using a model of Matsuzawa (1944) to simulate the trajectory of upthrown stones in the 1984 Western Nagano, Japan earthquake (M=6.8), anomalous high accelerations of 5 to 30 times of gravitational acceleration g, in the frequency range 5-10 Hz, were estimated from observed horizontal displacements of these boulders. The estimated ground accelerations were anomalous in the sense that no records are known of ground accelerations reaching 2 g.

There have been other reports in the literature of relatively rigid and compact objects that were apparently tossed into the air during strong ground shaking. As these were often interpreted, perhaps at times mistakenly, as evidence of over 1 g vertical acceleration, Newmark (Ref. 2) pointed out that the ground acceleration involved need not be over 1 g if the rigid object was considered to be elastically supported. Psycharis and Jennings (Ref. 3) showed complete separation of a rigid object from elastic ground to be conceivable even for purely horizontal excitation.

In this paper, the block-spring-dashpot model of Ref. 3 is extended, with spring and dashpot coefficients approximated from a theory of viscoelastic foundations (Ref. 4). Certain actual near-field accelerograms are considered as ground motion in numerical simulation of transient response of block. To attain ground accelerations of the order of 1 g, some of the accelerograms are scaled-up in amplitude. The projectile motion of upthrown block is traced until contact with the ground is regained. Thus any net displacement of the block relative to the ground, after upthrow, is calculated. Several cases are simulated and compared.

EQUATIONS OF MOTION

Before Uptthrow An upright circular cylinder of height $2H$, diameter $2R$ and uniformly distributed mass M is considered, as in Fig. 1(a). The block has three degrees of freedom as shown in Fig. 1(b): translations u and v , and small rotation θ relative to the static equilibrium position. This model is an extension from Ref. 3. The coefficients of springs and dashpots at the edges of the base of the block are approximated from Ref. 4, assuming full-contact condition; the vertical springs and dashpots are discretized representation of the rotational impedance of the base. The coefficients corresponding to the fundamental frequency of the elastically supported block are considered constant during the transient vibration. The ground is considered to accelerate vertically and horizontally.

Three types of contact may be obtained during the motion before upthrow. These are shown in Fig. 2. Linearized equations for each type of motion may be written in analogous forms, with only certain contact parameters different: e_1 and e_2 . Piecewise-linear nonlinear equations of motion may be written in matrix form as follows:

$$\begin{bmatrix} 1 & 1 & 0 \\ 1 & \frac{4}{3} + \frac{A^2}{4} & 0 \\ 0 & 0 & 1 \end{bmatrix} \begin{Bmatrix} \ddot{u} \\ H\ddot{\theta} \\ \ddot{v} \end{Bmatrix} + 2\zeta_v \omega_v \begin{bmatrix} e_1 Z \Omega & 0 & 0 \\ 0 & e_1 A^2 & e_2 A \\ 0 & e_2 A & e_1 \end{bmatrix} \begin{Bmatrix} \dot{u} \\ H\dot{\theta} \\ \dot{v} \end{Bmatrix} + \omega_v^2 \begin{bmatrix} e_1 \Omega^2 & 0 & 0 \\ 0 & e_1 A^2 & e_2 A \\ 0 & e_2 A & e_1 \end{bmatrix} \begin{Bmatrix} u \\ H\theta \\ v \end{Bmatrix} = - \begin{Bmatrix} \ddot{u}_g \\ \ddot{u}_g \\ \ddot{v}_g \end{Bmatrix} - \begin{Bmatrix} 0 \\ -e_2 Ag \\ (1-e_1)g \end{Bmatrix} \quad (1)$$

where the contact parameters (e_1, e_2) are (1,0), (0.5,-0.5), and (0.5,0.5) for full contact, left-edge uplift, and right-edge uplift, respectively. u_g and v_g are ground displacements. The other parameters in Eq. 1 are defined below.

$$\omega_j = \sqrt{2k_j / M} \quad \zeta_j = c_j / \sqrt{2k_j M} \quad j = u, v \quad (2), (3)$$

$$\Omega = \omega_u / \omega_v \quad Z = \zeta_u / \zeta_v \quad (4), (5)$$

$$A = R / H \quad (6)$$

Criteria for Uplift and Uptthrow Eq. 1 may be solved numerically at small time steps. The shift from one contact condition to another, and hence the change in contact parameters (e_1, e_2), may be detected by the following criteria. The current vertical dynamic translation v is compared with the static spring deformation v_s :

$$v_s = -Mg / 2k_v \quad (7)$$

and the rotation θ is compared with a critical angle θ_{cr} :

$$\theta_{cr} = \text{abs}(v+v_s) / R \quad (8)$$

There is full contact when v is less than $\text{abs}(v_s)$ and $\text{abs}(\theta)$ is less than θ_{cr} . Uplift of one edge is indicated when v is less than $\text{abs}(v_s)$ and $\text{abs}(\theta)$ is greater than θ_{cr} ; or when v is greater than $\text{abs}(v_s)$ and $\text{abs}(\theta)$ is greater than θ_{cr} . The left edge is uplifted when θ is positive; otherwise the right. Uptthrow is indicated when v is greater than $\text{abs}(v_s)$ and $\text{abs}(\theta)$ is less than θ_{cr} .

During Upthrow The block is in projectile motion during upthrow, while free-field motion is assumed for the ground. The block trajectory may be referred to the moving ground by the relative displacements \bar{u} , \bar{v} , and $\bar{\theta}$. If t denotes the time reckoned from start of upthrow, the explicit equations for the displacements may be written as follows.

$$\bar{u} = u_0 + \theta_0 H \cos \theta_0 + [\dot{u}_0 + \dot{\theta}_0 H \cos \theta_0] t - [\theta_0 H + \dot{\theta}_0 H t] \cos \{ \theta_0 + \dot{\theta}_0 t \} + [u_{g0} - u_g] \quad (9)$$

$$\bar{v} = v_0 - \theta_0 H \sin \theta_0 + [\dot{v}_0 - \dot{\theta}_0 H \sin \theta_0] t + [\theta_0 H + \dot{\theta}_0 H t] \sin \{ \theta_0 + \dot{\theta}_0 t \} + [v_{g0} - v_g] - \frac{gt^2}{2} \quad (10)$$

$$\bar{\theta} = \theta_0 + \dot{\theta}_0 t \quad (11)$$

where u_0 , v_0, \dots, u_{g0} and v_{g0} are displacements or velocities at the end of the last time interval governed by Eq. 1. End of upthrow, i.e. landing of the block on another location on the ground, may be detected as follows. To further allow a chance of large horizontal displacement, it is considered that the ground surface may be sloping downward at angle ψ , in the direction of the projectile (Fig. 3). Landing is indicated when \bar{v} approaches \bar{v}_{cr} :

$$\bar{v}_{cr} = R \sin \bar{\theta} - (\bar{u} + R \cos \bar{\theta}) \tan \psi \quad \bar{\theta} > \psi \quad (12)$$

$$\bar{v}_{cr} = - R \sin \bar{\theta} - (\bar{u} - R \cos \bar{\theta}) \tan \psi \quad \bar{\theta} < \psi \quad (13)$$

SIMULATIONS

Properties of Rigid Block and Viscoelastic Support Five example systems are considered, with block and soil properties as listed in Table 1. The examples are only slightly different from each other, with respect to block size R , aspect ratio A , ground slope ψ , or soil damping ratio ξ . The following properties are considered common: ratio of mass densities of soil and block ($m=0.5$); shear wave velocity in the soil ($c_s=100\text{m/s}$); and soil Poisson ratio ($\nu=0.33$).

Ground Motion Near-field accelerograms and their respective displacement histories as obtained by numerical integration, are adopted from three California earthquakes. (No records are available of the ground motions discussed in Ref. 1.) These are: NS and vertical components at El Centro of the 1940 Imperial Valley earthquake ($M_1=7.1$); 230° and vertical components at Array 7 and at Array 6 of the 1979 Imperial Valley earthquake ($M_1=6.6$); and 250° and vertical components at Anderson Dam Crest of the 1984 Morgan Hill earthquake ($M_1=6.2$). Except the 1940 records at El Centro, the accelerograms are shown in Fig. 4.

As inputs in the simulations, the amplitudes of ground motion records are scaled up in the proportions listed in Table 2, in order to attain acceleration levels between 1 g and 2 g. In one case (input I3), the vertical component is arbitrarily neglected. In another (I4), the amplitudes are left unscaled.

Predicted Upthrow Displacement The calculated net horizontal displacement of upthrown block is given in Table 3. All of the hypothetical input ground motions produce upthrow and net displacement of the smaller block; but the bigger block is hardly affected. Larger displacements are predicted when A is larger, i.e. when the block is stockier; when the ground is slightly sloping instead of flat; or when the soil damping is smaller.

Input I2 systematically produces larger displacement, although its acceleration peaks are not the greatest among the different inputs considered.

"Snap shots" of the simultaneous projectile motion of the block in system S3, and the ground motion according to input I2, are shown in Fig. 5, where it can be seen that as the block tosses up and leftward, the ground fortuitously moves rightward and down by significant amounts. In the process large net horizontal displacement of the block is produced.

DISCUSSION

The numerical simulations presented above have used several simplifying assumptions, and therefore can hardly be expected to fully predict and describe the phenomenon of upthrow. For instance, according to Ref. 5 no upthrow was actually reported around Array 6 (Huston Rd.) despite the simulation results above using actual amplitudes of Array 6 records (I4).

Instead, the present paper has demonstrated that the relation can be strongly nonlinear between net displacement of upthrown object and level of ground acceleration. Also, peculiar features may make certain ground motions more critical than others of similar acceleration level. Ground motion similar to the Array 7 records of the 1979 Imperial Valley earthquake, which has large pulses in the horizontal component of acceleration (Fig. 4), may be an example; input I2 in the simulations consistently leads to upthrow and significant net displacement.

Analysis similar to the method presented may lead to more realistic and believable estimates of strong accelerations at sites of reported upthrown rigid objects. Another recent study (Ref. 6) points to this direction.

REFERENCES

1. Umeda, Y., Kuroiso, A., Ito, K., Iio, Y. and Saeki, T., "High Accelerations in the Epicentral Area of the Western Nagano Prefecture Earthquake, 1984," J. Seism. Soc. Japan, 39, 2, 217-228 (In Japanese), 1986
2. Newmark, N., "Interpretation of Apparent Upthrow of Objects in Earthquakes," Proc. Fifth World Conf. Earthq. Eng., 2338-2343, 1973
3. Psycharis, I. and Jennings, P., "Upthrow of Objects due to Horizontal Impulse Excitation," Bul. Seism. Soc. America, 75, 2, 543-561, 1985
4. Veletsos, A. and Verbic, B., "Vibration of Viscoelastic Foundations," Earthq. Eng. Struct. Dyn., 2, 87-102, 1973
5. Sharp, R. V., Private communication, 1987
6. Ohmachi, T. and Arai, Y., "Earthquake-induced Jumps of Objects Partly Embedded in the Ground," JSCE J. Struct. Eng., 33A, 11pp. (In Japanese), 1987

Table 1 Example Block-Soil Systems

System	R (cm)	A	ψ (deg)	ξ
S1	10	1.0	20	0.1
S2	10	1.0	20	0.2
S3	10	1.0	0	0.1
S4	10	0.75	20	0.1
S5	25	1.0	20	0.1

Table 2 Simulated Input Ground Motions

Input	Source Record	$\max \ddot{u}_g$	$\max \ddot{v}_g$
I1	El Centro x 3	1.04 g	-0.63 g
I2	Array 7 x 2	0.92 g	-1.02 g
I3	I2 without v	0.92 g	--
I4	Array 6	-0.44 g	1.69 g
I5	Anderson x 2	-1.26 g	0.40 g
I6	Anderson x 3	-1.89 g	0.60 g

Table 3 Predicted Net Horizontal Displacement (cm)

	S1	S2	S3	S4	S5
I1	20.3	11.4	18.3	7.9	--
I2	75.2	39.1	64.3	27.8	10.9
I3	23.9	12.3	20.1	12.1	--
I4	24.7	14.6	21.0	9.3	--
I5	15.1	9.7	14.3	6.2	--
I6	23.0	14.5	21.3	9.4	3.2

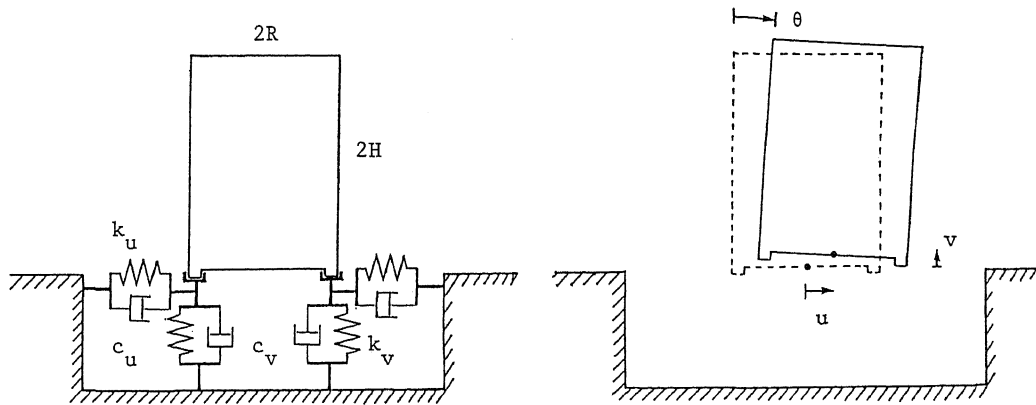


Fig. 1 (a) Unbonded Rigid Block. (b) Three Degrees of Freedom.

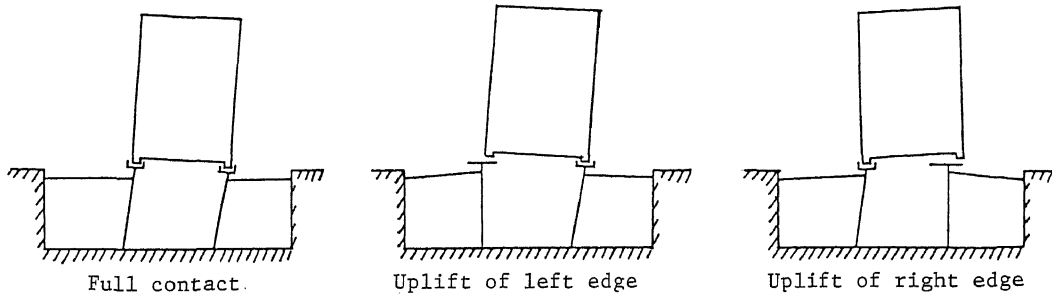


Fig. 2 Three Types of Contact Condition

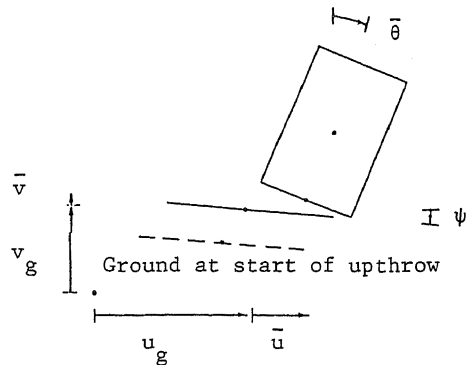


Fig. 3 Landing of Upthrown Block

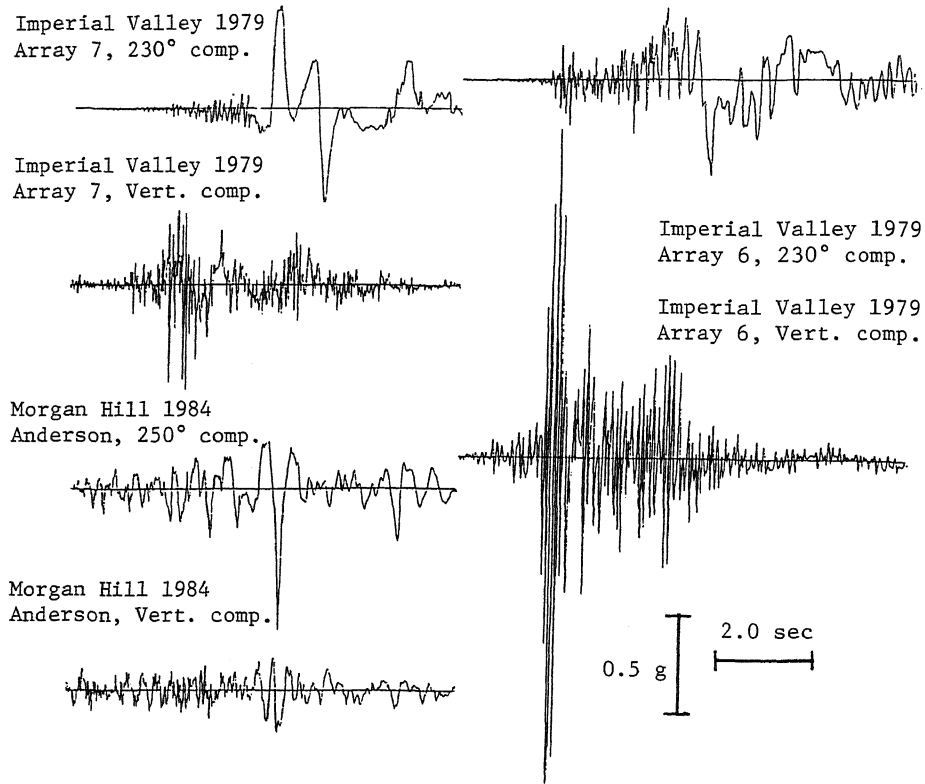


Fig. 4 Acceleration Records Used For Simulating Ground Motion (See Table 2)

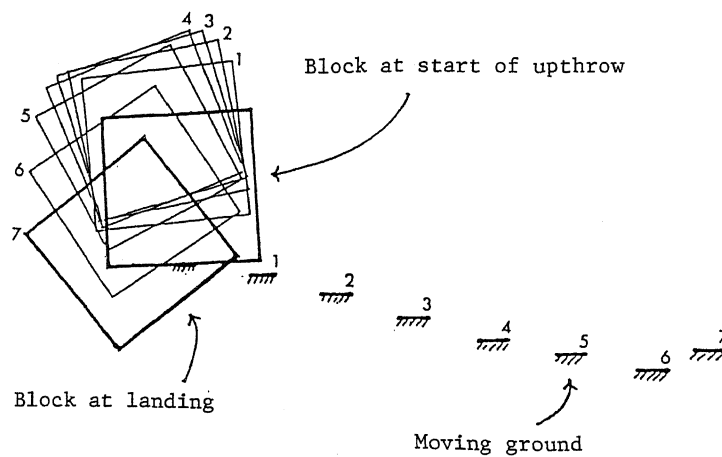


Fig. 5 Relative Positions of Uprthrown Block and Moving Ground (S3 and I2)